THE FLEUXRAL BEHAVIOR OF LIGHTWEIGHT CONCRETE SLABS REINFORCED BY GFRP

Doha A.Ahmed*, Gouda M. Ghanem*, Waleed A.Abdelfattah*
* Civil Engineering Department, Faculty of Engineering- Mataria, Helwan university, Egypt.

Abstract

In this study, an innovative idea for a lightweight concrete slab reinforced by GFRP and testing the flexural behavior of these slabs. Six slabs were tested, each consisting of two materials: lightweight concrete (LC) and glass fiber-reinforced (GFRP) sections. The flexural test was due to three parameters: the spacing between the GFRP sections, The geometry of the GFRP cross-section, and the use of stiffeners. The ultimate load capacity of the slab was increased by 22.4 % when the distance between GFRP sections decreased from 350 to 233. Changing the geometry of the GFRP cross-section area from I to U increased the ultimate load by 20.2%. Changing the shape from I to T led to a decrease in the maximum load by 15.5%. Increasing the load depends on increasing the inertia of the cross-section. Using glass fiber stiffeners between GFRP increased maximum load by 3% .

I. INTRODUCTION

Concrete's disadvantaged tensile capacity frequently leads to brittle breakdown without notice. One solution is introducing fibers and enhancing concrete failure's tensile strength (TS) behavior (Al-Kharabsheh et al., 2022). These materials have been widely used in various industries, including automotive, marine, aviation, railway, sports, and wind. Over 20% of all FRPs manufactured are utilized globally in the civil and building industries. (Al-Salloum and Almusallam, 2003). Bridge structures have frequently used fiber-reinforced polymer (FRP) composites in recent years. The benefits of repairing and strengthening are already well-known. Increasingly, new structures are being built using

only FRP or hybrid FRP structures (Ali et al., 2021). The advantages of FRP composites, such as their low self-weight, high strength, high degree of free shaping, and strong resistance to corrosion and fatigue, are primarily responsible for this growth. In addition, compared to concrete slabs, building elements, such as the waterproofing layer, could be more easily created. This method also emphasized some scientific weaknesses and the costly expenses that limited its wide use (Keller, Schaumann, and Vallée, 2007). Research on glass fibers was done in the early 1950s in the United States, the United Kingdom, and Russia. Glass fibers were researched in Russia and employed in the building business. However, this kind of fiber was discovered to be vulnerable to alkaline assaults. 1950s. Since the early 1960s, there has been a surge in interest in fiber-reinforced concrete, which was a critical moment in the history of FRC. Later, in the late 1970s and early 1980s, fracture toughness was established as testing equipment and analytical processes grew more quantitative and qualitative. Even after more than three decades of study in this sector, the main advantage of FRC is its great fracture toughness. The 1982 Miyun Bridge in China was the first hybrid FRP-concrete road traffic bridge. The supported two-lane bridge was constructed out of a 10 cm thickness reinforced concrete slab and six hexagonal sandwich FRP box girders. Shear bolts are used to join the slab to the box girders. Then, a lightweight hybrid beam was designed in the 1990s (Keller, Schaumann and Vallée, 2007). It was constructed of a GFRP filament-tied box section with a CFRP strap on the bottom flange functioning as the tension zone and a concrete layer on the top side working as the compression zone. A two-component epoxy adhesive was utilized for bonding the concrete with the GFRP flange (Keller and Vallée, 2005), (Deskovic, Meier, and Triantafillou, 1995), and (Li et al., 2015). (Schaumann, Vallée and Keller, 2008) Conducted direct load transmission tests on hybrid short-span beam specimens for an experimental bridge deck. The sandwich structure comprises a lightweight concrete (LC) core, a thin layer of ultra-high performance reinforced concrete on top, and a bottom skin made of a fiber-reinforced polymer composite (FRP) sheet with T-upstands. Due to pure mechanical interlocking, the maximum loads of specimens with adhesively bonded FRP LC interfaces were much more significant than those of equivalent unbonded.

II. EXPERIMENTAL PROCEDURE

A. Material properties

The materials used to cast the reinforced Lightweight aggregate concrete are Portland cement, coarse aggregates, natural sand, silica fumes, clean water, superplasticizer, and polypropylene fibers. The mixes were designed to develop an average cubic strength of 23 MPa after 90 days. The mixed design of the LC is presented in Table 1. Six cylinders of 320 mm in length and 160 mm in diameter were cast with the slabs for the mixture. Furthermore, eight cubes with 100 mm length were cast together with the slabs. The cylinders and cubes were stored in a climate room for 28 days at 20 °C and 95% relative humidity. The rounded average densities of 17.5 and 18.7 KN/m3 were obtained from cylinders and cores. The results are summarized in Table 2 (average values and standard deviation). Table 3. gives the tensile strength and Young's modulus of the GFRP. Table 4. Shows the mechanical properties of polypropylene.

Table1. Mixture of LC concrete

Cement (Kg)	Silica Fume (kg)	Coarse Agg. (kg)	Fine Agg. (kg)	Polys. Foam (L)	Super Plasticizer (L)	Water (L)	Fiber (kg)
450	40	630	630	330	13.5	139	139

Table2. Mechanical properties of LC mix

Concrete	Density (kg/m3)	Compression strength of cubes after 28 days (MPa)	Compression strength of cylinder after 28 days (Mpa)	Tensile strength (Mpa)
LC	18.1	23.5	17.9	1.97

Table3. Mechanical properties of GFRP

Mechanical properties of GFRP	
Ultimate tensile stress (Mpa)	465
Modulus of elasticity (Mpa)	24000

A. Slabs description

The experimental program consisted of six hybrid lightweight reinforced concrete slabs that were prepared to test the flexure behavior of slabs under different variables. All test specimens have the same concrete dimensions (the length of 1600mm and the width of 800 mm). Specimens were divided into three groups. Group one aimed at studying the effect of Changing the geometry of GFRP. It contains three specimens (SI350, S⊥350, and SU350). These specimens contain different geometry of GFRP sections but have the same total Area. All dimensions are Shown in figure1. The specimens have an equal spacing of 350 mm in the longitudinal direction, as shown in Figures 2,3 and 4.

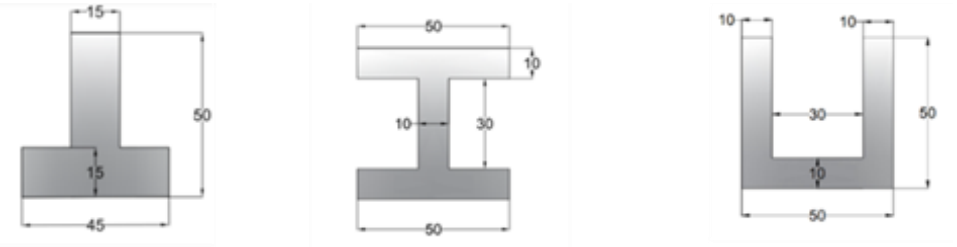

Fig. 1. The dimensions of different GFRP cross sections in mm.

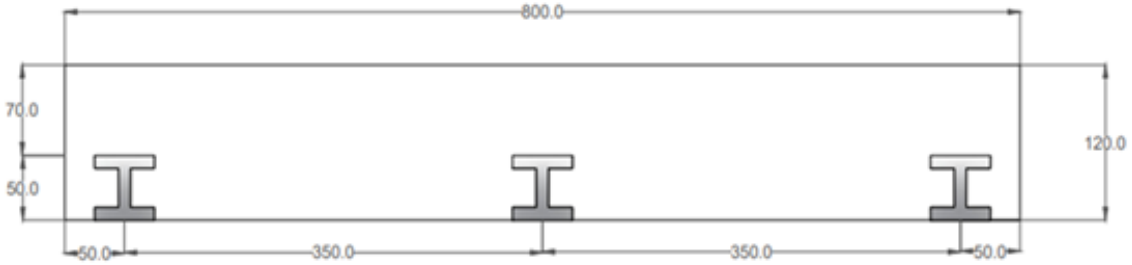

Fig. 2. Cross section of SI350.

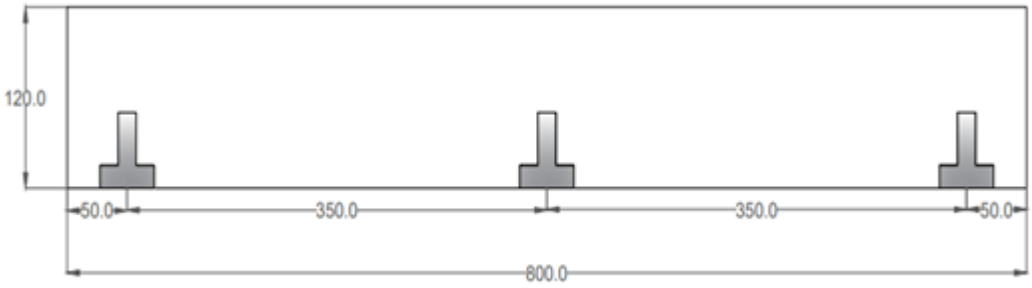

Fig. 3. Cross section of ST350.

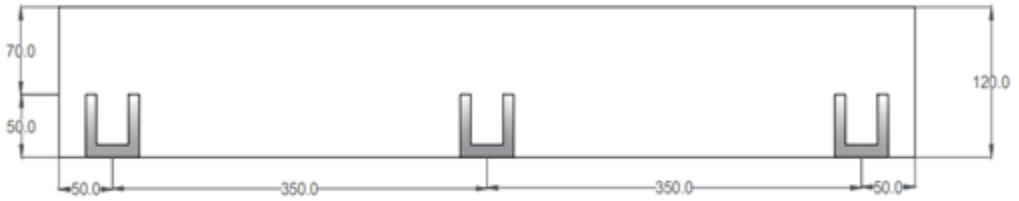

Fig. 4. cross section of SU350.

Group two aimed to study the effect of changing the spacing between glass fiber sections. It consisted of two specimens reinforced with GFRP I-sections. The Spacing between I-sections is 233mm (CL to CL) in specimen I233, as shown in Figure 5, while the spacing is 350 in Specimen S1350, as shown in Figure 6.

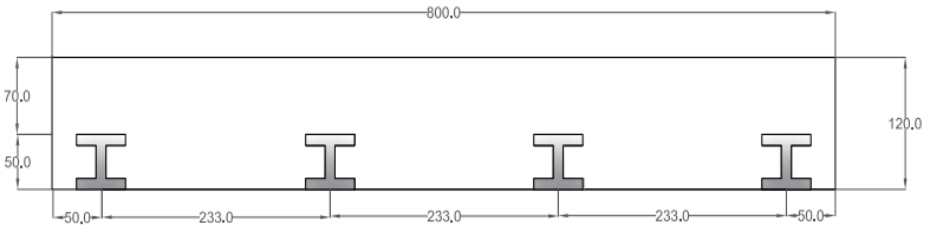

Fig. 5. Cross section of SI350.

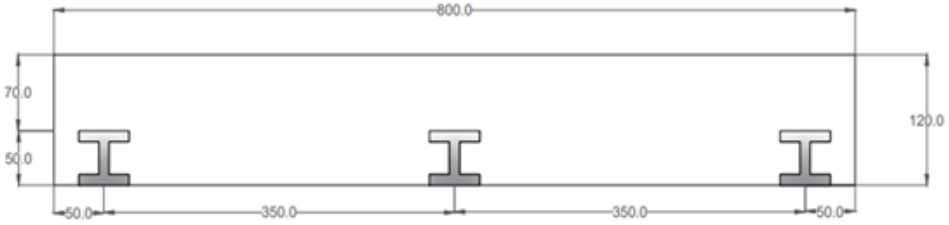

Fig. 6. Cross section of SI350.

Group three aimed at studying the effect of using stiffeners. It contains two specimens, ST350S, and SI350S. All dimensions are in Figures 7 and 8.

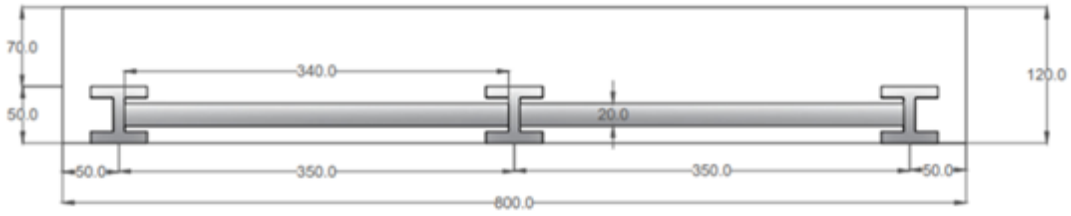

Fig. 7. Cross section of SI350S.

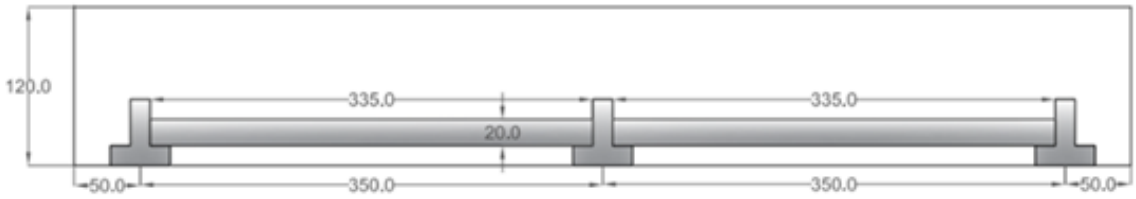

Fig. 8. Cross section of SI350S.

III. Experimental procedures

A. Experimental set-up and instrumentation

To measure a gauge length of 600 mm, two linear voltage displacement transducers (LVDT) were mounted to the specimens on two opposing sides of their mid-height for all slabs. The LVDTs were linked to a data acquisition system operated by a computer. This system captures measurements at a rate of two readings per second, including loads from the load cell and strains from the electrical strain gauges. Throughout the test of phase two specimens, electrical strain gauges (HPM) of 10 mm length and 120 Ohm resistance were utilized to measure steel stresses. In this regard, two HPM electrical strain gauges were attached to the GFRP Sections, one in the center and one outside the GFRP. Each strain gauge bonded in the connection between the web and the lower flange. Before the reinforcement was placed in the formwork, the strain gauges were bonded to the reinforcement GFRP sections using a quick setting epoxy as an adhesive, as shown in Figures (9&10).

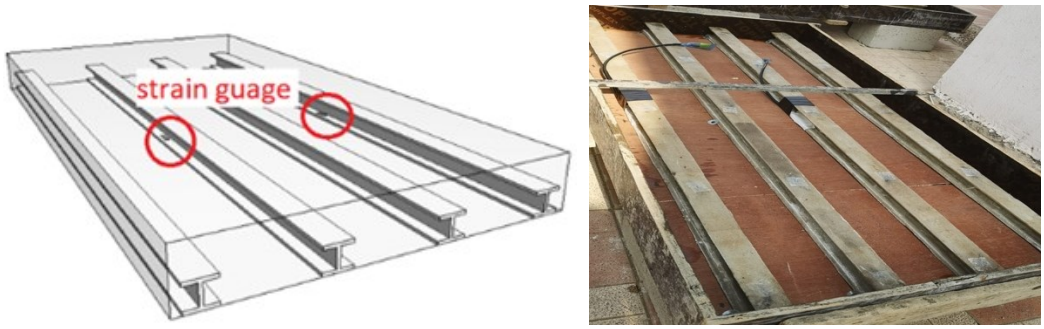

Fig. 9. Installation of the strain gauge in SI233.

Fig. 10. Installation of the strain gauge in ST350S.

B. Slab Manufacturing

After being instrumented with strain gages, the FRP components were integrated into a wooden formwork in the lab. To strengthen the bond between the FRP and the concrete, epoxy adhesive was applied to the FRP components, and the surfaces were roughened.

C. Test Set-up

To study the flexural behavior of the slabs, the structural element should not be subjected to any other stresses, such as shear. Therefore, the test was prepared so that two loads are concentrated at equal distances from the centroid axis of the slab, as shown in Figure 11. The test was prepared by placing a steel beam supported from the sides with two solid steel bars made of iron, each rod on one side of the steel beam. Finally, the slab is placed under the two bars so that each rod represents a load center that affects the slab, as shown in figure 12.

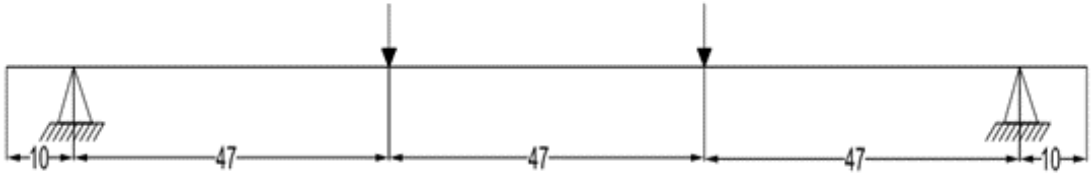

Fig.11. The test spacing in the slab in cm.

Fig. 12. Test set-up.

IV. RESULTS AND DISCUSSION

The test results are presented in four responses: ultimate vertical load, Mode of failure, Strain behavior, and Specimen deformation. Table 4. Shows a summary of all results.

Table 4. The experimental results of the tested slabs

Specimen	First Crack load (KN)	Ultimate Load (KN)	Mid-section strain (mm/mm)	Edge-section strain (mm/mm)	Deflection at mid-span Δ_1 (mm)	$\frac{P_{cr}}{P_{ult}}$
SI233	**48.9**	**112**	**0.0077**	**0.0065**	**9.15**	**0.43**
SI350	**33.5**	**91.5**	**0.007**	**0.0051**	**5.5**	**0.36**
ST350	**28.6**	**77.3**	**0.0071**	**0.0047**	**4.1**	**0.37**
SU350	**49**	**110**	**0.0088**	**Failed**	**8.74**	**0.44**
SI350S	**39.4**	**94**	**0.0065**	**0.0051**	**5.5**	**0.41**
ST350S	**32.3**	**79**	**0.0067**	**0.005**	**10**	**0.40**

Figures (13-18) show the cracks pattern of the tested specimens SI233, SI350, ST350, SU350, SI350S, and ST350S. In the figures, each crack is marked by a line

representing the direction of the crack. The first crack appeared in the tension side in the middle of the specimens parallel to the loading line. Then, several parallel cracks spread with the load increase. At a certain loading level, the concrete cover under the GFRP sections tends to separate from the section due to weak debonding between concrete sections. Finally, the specimen failed when the ultimate load was achieved, and a remarkable slippage occurred.

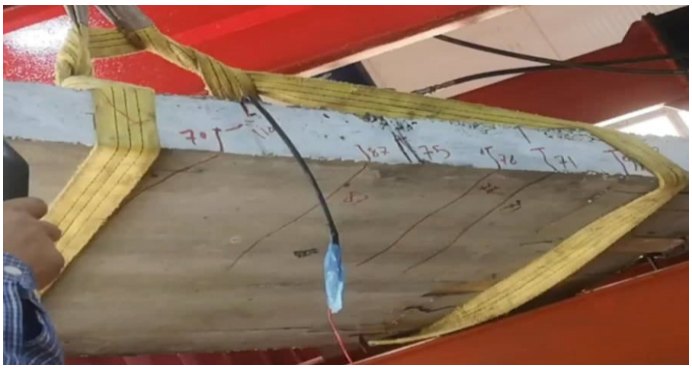

Figure 13. The crack pattern of Specimen SI233.

Figure 14. The crack pattern of Specimen SI350.

Figure 15. The Crack Pattern of Specimen ST350.

Figure 16. The Crack Pattern of Specimen SU350.

Figure 17. The crack pattern of Specimen SI350S.

Figure 18. The Crack Pattern of Specimen ST350S.

Changing spacing between GFRP (S) is a significant parameter affecting the ultimate load capacity and the cracking load, as shown in Table 4. The behavior can be presented by comparing the test slabs' SI233 and SI350 results. The two specimens had the same cross-section area. Specimen SI233 had maximum ultimate comparison with the other specimen. Decreasing the spacing between GFRP increases the ultimate load. The

relation between the load and the strain of the two specimens is shown in Figure 19. the relation between the load and displacement of the two specimens is shown in Figure 20.

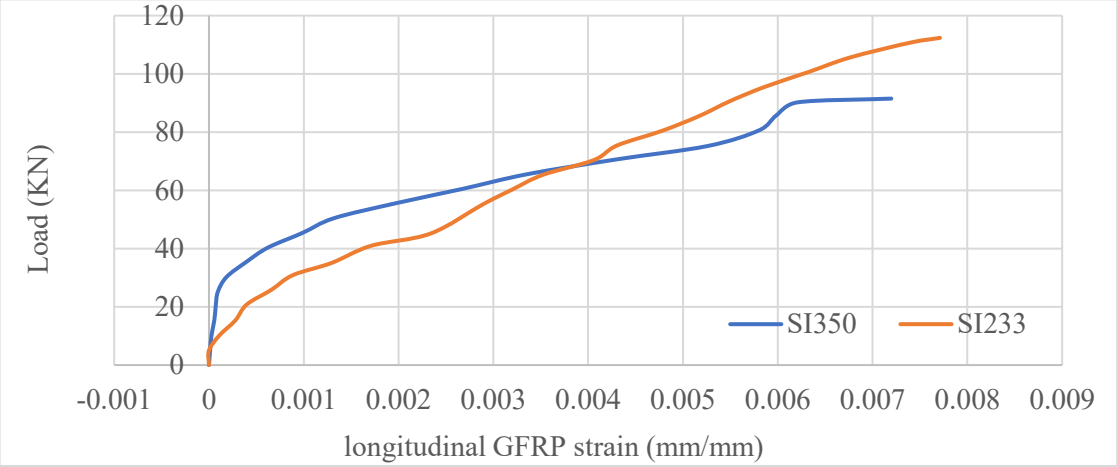

Fig.19. Load versus middle section longitudinal GFRP strain of Specimens SI350& SI233.

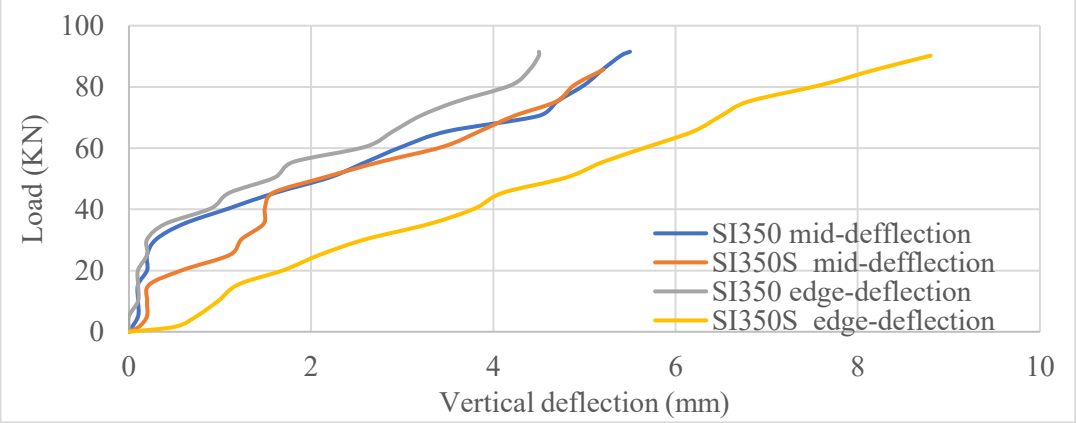

Fig.20. Load versus vertical deflection at LVDTs locations in the middle and edge sides of Specimens SI350 & SI233.

Changing GFRP geometry is a significant parameter affecting the ultimate load capacity and the cracking load. The behavior can be presented by comparing the test slabs SI350, ST350, and SU350 results. The three specimens had the same amount of glass fiber, so the difference would be in the inertia. Specimen SU350 had maximum ultimate load compared with other specimens. The (U) has the maximum inertia of the other shapes (I

and T). It could be concluded that increasing the load depends on increasing the inertia of the cross section. The relation between the load and the strain of the three specimens is shown in Figure 21.

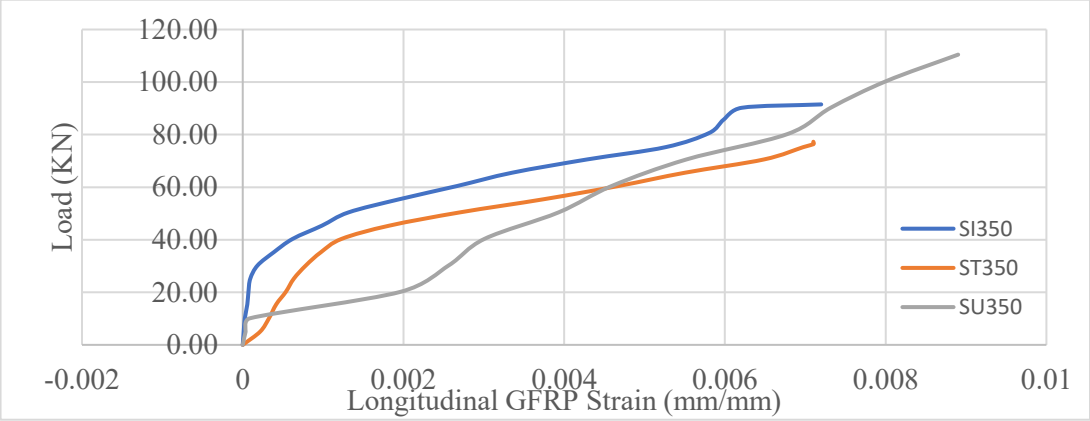

Fig.21. Load versus middle section longitudinal GFRP strain of Specimens SI350, ST350 and SU350.

The results of using glass fiber stiffeners between GFRP sections did not meet the expectation it had a little effect on the ultimate load and the cracking load, as shown in Table 4. The behavior of the slabs can be presented by comparing the results of tested slabs SI350 and SI350s by comparing ST350 and ST350. Specimen SI350S and ST350S had maximum ultimate comparison with SI350 and ST350. The relation between the load and the strain of the four specimens is shown in Figures 22 and 23, and the relation between the load and displacement of the two specimens is shown in Figures 24 and 25.

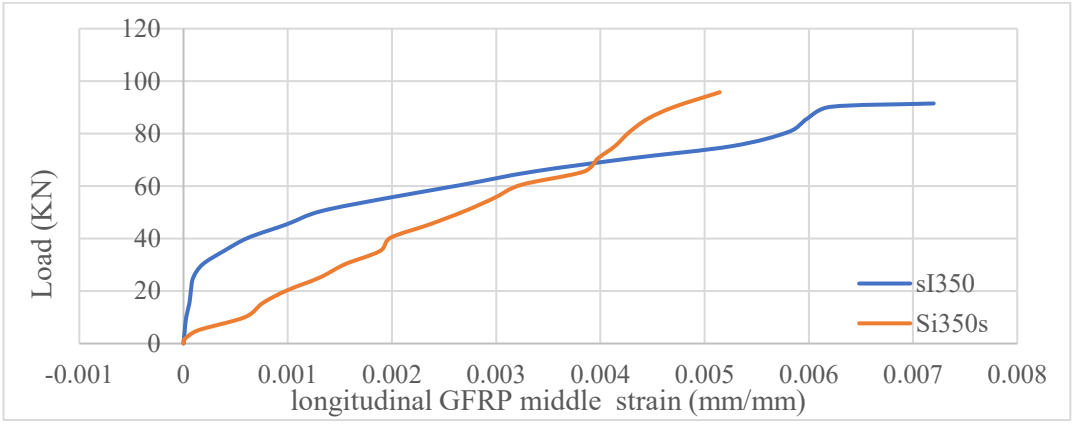

Fig.22. Load versus middle section longitudinal GFRP strain of Specimens SI350 and SI350S.

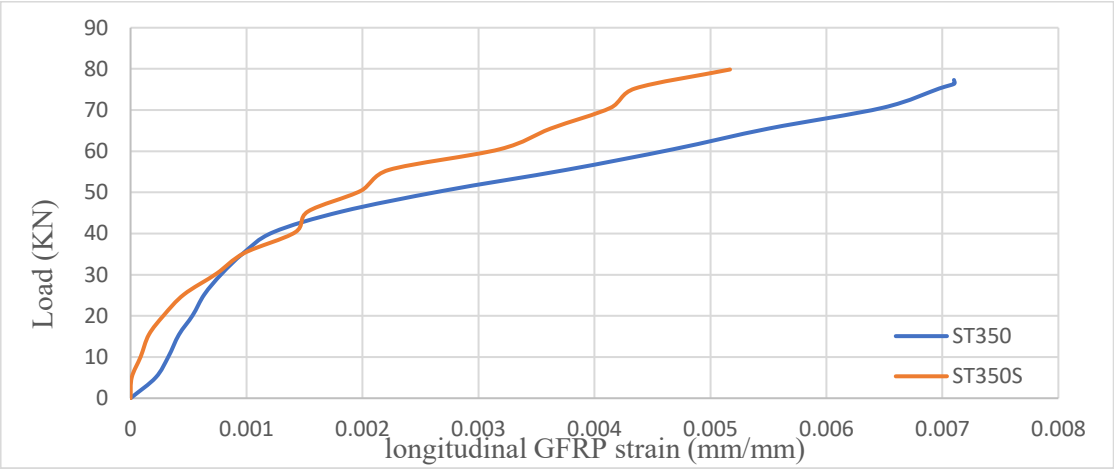

Fig.23. Load versus middle section longitudinal GFRP strain of Specimens ST350 and ST350S.

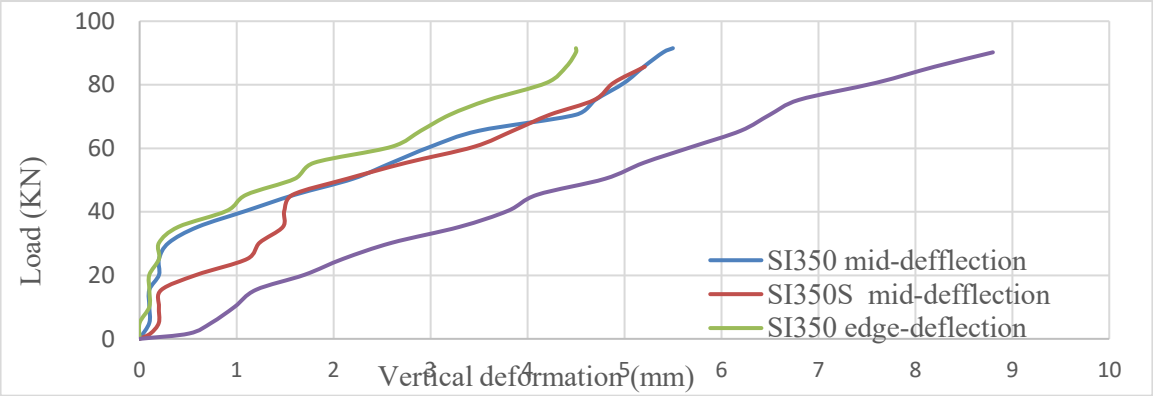

Fig.24. Load versus vertical deflection at LVDTs locations in the middle and edge sides of Specimens SI350 & SI350S.

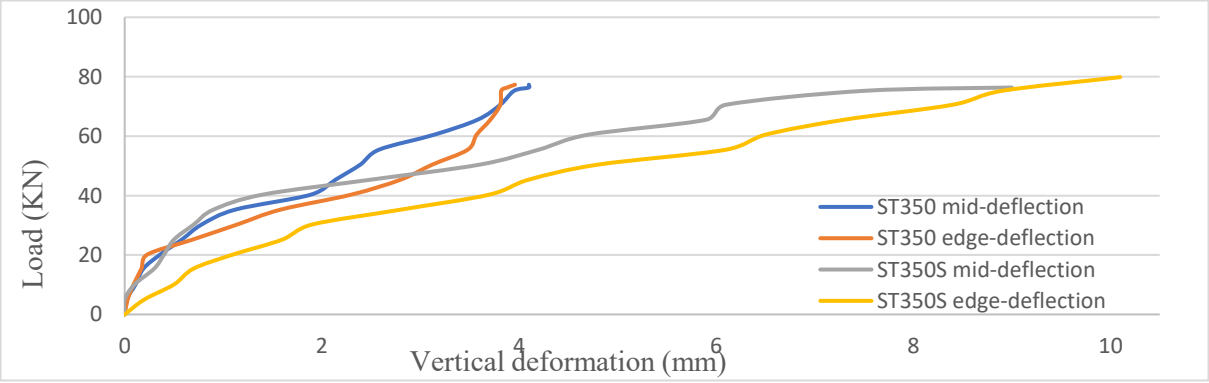

Fig.25. Load versus vertical deflection at LVDTs locations in the middle and edge sides of Specimens ST350 & ST350S.

V. CONCLUSION

This research is mainly concerned with studying the flexure behavior of hybrid GFRP-reinforced concrete slabs experimentally. The investigation was undertaken on six specimens until failure. The achieved compressive strength of the tested concrete cubes was 23 MPa.

The evaluation of slabs performance was based on the main parameters: the effect of changing the spacing between GFRP sections, the effect of changing the geometry of GFRP sections, and the effect of using stiffeners between the GFRP sections.

Based on the presented study, the main conclusions are:

1. Increasing the spacing between GFRP sections reduced the ultimate load capacity of the slab. Reducing the spacing from 350 to 233 led to an increase in the ultimate load by 22.4%.
2. Different cross-section areas led to different inertia. However, with the same amount of glass fiber and the same volume of specimens, the ultimate load is arranged in descending order due to the inertia of GFRP sections. Changing the GFRP cross-section area from I to U increased the cracking and ultimate load by 46% and 20.2%, respectively. Changing the shape from T to I led to an increase in the cracking and ultimate loads by 17.1% and 18.3%, respectively.
3. The results of using glass fiber stiffeners between GFRP sections did not meet expectations. It affected the ultimate load capacity. It leads to an increase in slab ultimate load by 3%.

VI. REFERENCES

(Ali et al. 2021). Ali, H.T. et al. 2021. Fiber-reinforced polymer composites in bridge industry. Structures 30, pp. 774–785. Available at: http://dx.doi.org/10.1016/j.istruc.2020.12.092.

(AL-Kharabsheh et al. 2022). AL-Kharabsheh, B.N., Arbili, M.M., Majdi, A., Alogla, S.M., Hakamy, A., Ahmad, J. and Deifalla, A.F., 2022. Basalt Fibers Reinforced Concrete: Strength and Failure Modes. Materials 2022, 15, 7350.

(Al-Salloum and Almusallam, 2003). Al-Salloum, Y.A. and Almusallam, T.H. 2003. Rehabilitation of the Infrastructure Using Composite Materials: Overview and Applications. Journal of King Saud University - Engineering Sciences 16(1), pp. 1–20.

(Amadio et al. 2004). Amadio, C., Fedrigo, C., Fragiacomo, M. and Macorini, L., 2004. Experimental evaluation of effective width in steel–concrete composite beams. Journal of Constructional Steel Research [online], 60 (2), 199–220

(Bate 1979). Bate, S.C.C. 1979. Guide for structural lightweight aggregate concrete: report of ACI committee 213. International Journal of Cement Composites and Lightweight Concrete 1(1), pp. 5–6.

(Deskovic, Meier and Triantafillou, 1995). Deskovic, N., Meier, U. and Triantafillou, T. C., 1995. Innovative Design of FRP Combined with Concrete: Long-Term Behavior. Journal of Structural Engineering [online], 121 (7), 1079–1089.

(Keller and Vallée 2005). Keller, T. and Vallée, T., 2005. Adhesively bonded lap joints from pultruded GFRP profiles. Part I: stress–strain analysis and failure modes. Composites Part B: Engineering [online], 36 (4), 331–340.

(Keller, Schaumann and Vallée, 2007). Keller, T., Schaumann, E., & Vallée, T. (2007, March). Flexural behavior of a hybrid FRP and lightweight concrete sandwich bridge deck. Composites Part A: Applied Science and Manufacturing, 38(3), 879–889.

(Schaumann, Vallée and Keller, 2008). Schaumann, E., Vallée, T., & Keller, T. (2008, March). Direct load transmission in hybrid FRP and lightweight concrete sandwich bridge deck. Composites Part A: Applied Science and Manufacturing, 39(3).

(Lasheen, Shaat and Khalil, 2016). Lasheen, M., Shaat, A. and Khalil, A. (2016) "Behaviour of lightweight concrete slabs acting compositely with steel I-sections," Construction and Building Materials, 124, pp. 967–981. doi 10.1016/j.conbuildmat.2016.08.007.

(Li et al., 2015). Li, L., Fan, J., Jiang, Y. and Zhang, Y., 2015. Improved Strength Model of FRP-Confined Concrete in Rectangular Columns. International Journal of Structural and Civil Engineering Research [online]. 478–487.

(Meyer and Kahn 2002). Meyer, K.F. and Kahn, L.F. 2002. Lightweight Concrete Reduces Weight and Increases Span Length of Pretensioned Concrete Bridge Girders. PCI Journal 47(1), pp. 68–75. Available at: http://dx.doi.org/10.15554/pcij.01012002.68.75.

(Nie, Tian and Cai, 2008). Nie, J.-G., Tian, C.-Y. and Cai, C. S., 2008. Effective width of steel–concrete composite beam at ultimate strength state. Engineering Structures [online], 30 (5), 1396–1407.

(Weigler and Karl 1980). Weigler, H. and Karl, S., 1980. Structural lightweight aggregate concrete with reduced density— lightweight aggregate foamed concrete. International Journal of Cement Composites and Lightweight Concrete [online], 2 (2), 101–104.